Performance analysis of cascaded doubly fed induction generator with matrix converter for wind power conversion systems

Amar Maafa, Abdelghani Yahiou, Mellah Hacene, Hamza Sahraoui

Studies in Engineering and Exact Sciences
ISSN: 2764-0981

Performance analysis of cascaded doubly fed induction generator with matrix converter for wind power conversion systems

Análise de desempenho do gerador de indução duplamente alimentado em cascata com conversor matricial para sistemas de conversão de energia eólica

Análisis de desempeño del generador de inducción doble alimentado en cascada con convertidor matricial para sistemas de conversión de energía eólica

DOI: 10.54021/seesv5n2-578

Originals received: 10/25/2024
Acceptance for publication: 11/19/2024

Amar Maafa
PhD in Electrical Engineering
Institution: Engineering Department, Faculty of Sciences and Applied Sciences, University of Bouira
Address: Béjaïa, Algeria
E-mail: omaafa@univ-bouira.dz

Abdelghani Yahiou
PhD in Electrical Engineering
Institution : Engineering Department, Faculty of Sciences and Applied Sciences, University of Bouira
Address: Tala Oulili, Bouandas, Sétif, Algeria
E-mail : abdelghani.yahiou@univ-bouira.dz

Mellah Hacene
PhD in Electrical Engineering
Institution: Engineering Department, Faculty of Sciences and Applied Sciences, University of Bouira
Address: Bouira, Algeria
E-mail: h.mellah@univ-bouira.dz

Hamza Sahraoui
PhD in Electrical Engineering
Institution: Electrical Engineering Department, Universite Hassiba Benbouali de Chlef
Address: Chlef, Algeria
E-mail: h.sahraoui@univ-chlef.dz

ABSTRACT
The purpose of this research study is to investigate the performance of a cascaded doubly fed induction generator (CDFIG) that is integrated with a matrix converter (MC) while operating at various speeds and while connected to the grid. The operating efficiency and stability of the CDFIG system under a variety of load scenarios are the primary factors that are investigated in this study. The MC is able to promote seamless energy conversion by utilizing the control methodologies that have been proposed, which ultimately improves the overall performance of the system. For the purpose of achieving the desired level of power delivery to the grid, the control performance will be improved via the utilization of a matrix converter (MC). Additionally, the system's reliability and efficiency will be improved through the utilization of the benefits that the CDFIG has in comparison to the DFIG. Results of the simulation show that there are considerable gains in power quality and fault tolerance, which highlights the potential of this arrangement for applications involving renewable energy, particularly in systems that generate fluctuating wind power.

Keywords: Matrix Converter. Cascaded Doubly Fed Induction Generator (CDFIG). Wind Energy. Energy Management.

RESUMO
Este artigo de pesquisa investiga o desempenho de um gerador de indução duplamente alimentado em cascata (CDFIG) integrado com um Conversor Matricial (MC) em condições de operação em velocidade variável e conexão à rede. O estudo foca na eficiência operacional e estabilidade do sistema CDFIG sob diversas condições de carga. Utilizando as estratégias de controle propostas, o MC facilita a conversão de energia de maneira contínua, aprimorando o desempenho geral do sistema. O objetivo é garantir a entrega de potência necessária à rede, melhorando o desempenho de controle com o uso do conversor matricial (MC) e aumentando a confiabilidade e eficiência do sistema ao explorar as vantagens do CDFIG em comparação ao DFIG. Resultados de simulação demonstram melhorias significativas na qualidade da energia e na tolerância a falhas, destacando o potencial dessa configuração para aplicações de energia renovável, especialmente em sistemas de geração eólica de potência variável.

Palavras-chave: Conversor Matricial. Gerador de Indução Duplamente Alimentado em Cascata (CDFIG). Energia Eólica. Gerenciamento de Energia.

RESUMEN
Este artículo de investigación analiza el desempeño de un generador de inducción doblemente alimentado en cascada (CDFIG) integrado con un Convertidor Matricial (MC) en condiciones de operación a velocidad variable y conectado a la red. El estudio se centra en la eficiencia operativa y la estabilidad del sistema CDFIG bajo diversas condiciones de carga. Utilizando las estrategias de control propuestas, el MC facilita una conversión de energía continua, mejorando el rendimiento general del sistema. El objetivo es lograr la entrega de potencia requerida a la red, mejorando el rendimiento del control mediante el uso del convertidor matricial (MC), y aumentar la fiabilidad y eficiencia del sistema aprovechando las ventajas del CDFIG en comparación con el DFIG. Los resultados de simulación demuestran mejoras significativas en la calidad de la

energía y la tolerancia a fallos, destacando el potencial de esta configuración para aplicaciones de energía renovable, particularmente en sistemas de generación eólica con potencia variable.

Palabras clave: Convertidor Matricial. Generador de Inducción Doble Alimentado en Cascada (CDFIG). Energía Eólica. Gestiónde la Energía.

1 INTRODUCTION

Given the urgent need to develop clean, inexpensive and sustainable energy systems, the current interest in wind energy is growing, that we can trust in the long term (Barote *et al*., 2010) - (Maafa *et al*., 2016). Due to its similar brushless and copper ringless behavior, CDFIG is a good candidate to replace DFIG, this is of course due to the high level of reliability that some applications require (Maafa *et al*., 2016) – (Admowicz zt al., 2008).

The trend and increasing interest in recent years has been around schemes for converting direct energy, using AC–AC converters (Tail *et al*., 2013). Among the AC-AC converters we find the three-phase matrix converter. It consists of nine two-way switches .Thus, the power flow can be reversed through the converter. The energy output must be equal to the instantaneous energy input, since there is no means of storing energy, of course, assuming an ideal loss-free switch. However, equality between the reactive power output and the reactive power input should not be considered. Furthermore, it may be said that the phase angle between the input and output voltages and currents is controllable and need not match. In addition, the frequency and form are different and independent of each side (Mohan *et al*., 2003).

Venturini and Alesina's work is considered among the first extensive research in the field of matrix converters (MC). In accordance with the duty-cycle matrix method, this method also represents it by quantities in the time domain (Alsina *et al*., 1989). The representation of a vector space in a complex space is considered as one of the bases for the modulation solution known as SVM (Benachour *et al*., 2017) – (Yue *et al*., 2007). There are two developed approaches in the literature, direct SVM (Casadei *et al*., 1993) and indirect (Huber *et al*., 1995). The indirect space vector modulation (SVM) technique is examined in this work. In

this pa work, the indirect space vector modulation (SVM) approach is studied.

A modulation strategy known as indirect vector space modulation separates the control of the output voltage and the input currents into two steps. To fully control the entire matrix converter, two transfer matrixes are required, and the well-known space vector modulation (SVM) method is exploited to the correction and inversion stages respectively (Yue *et al*., 2007).

The work presented in this paper highlights a developed and sophisticated model that allows us to simulate the behavior and operability of a variable speed wind generator (VSWG) connected to the power system. The device under study is composed of CDFIG such that there are two stator that are connected to the network, the first is connected directly, and the second is connected via a matrix converter. To ensure good control of the exchange of active and reactive power directions between power system network and the wind power generator, this paper also presents a vector-control strategy, in addition of to the PI regulator, the power control algorithm will be presented. As a final part of the paper, the use of numerical simulation will be presented to provide a study of the device. Figure 1 shows a synoptic scheme of the studied device. The CDFIG system incorporates a matrix converter to manage the bidirectional power flow, replacing traditional rectifier-inverter setups. A PI regulator are implemented to optimize the converter's performance, ensuring minimal harmonic distortion and improved power factor.

Figure 1. Studied device scheme

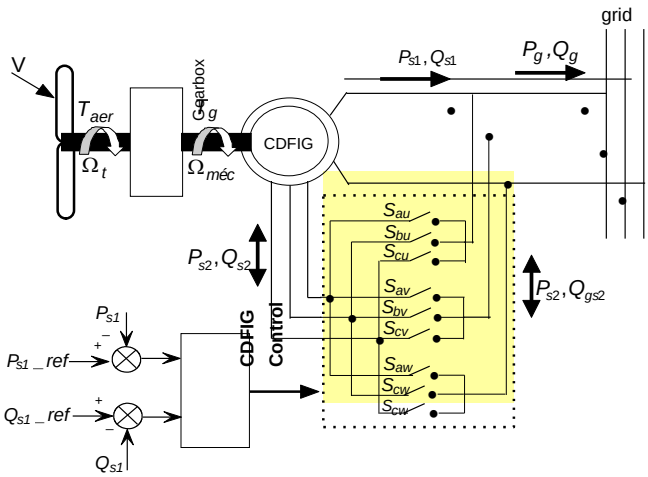

Source: Authors

2 PRINCIPLES OF MATRIX CONVERTER

To allow the connection of output phases A, B, C to any of the input phases a, b, c, a direct matrix converter consisting of nine bidirectional switches is used. As shown in Figure 2, there are three input phases connected to three switches set connected to each output phase. The fixed input voltage amplitude and fixed frequency are required to calculate the variable frequency and the sinusoidal output voltage amplitude (Yue *et al*., 2007).

Figure 2. Matrix converter topology

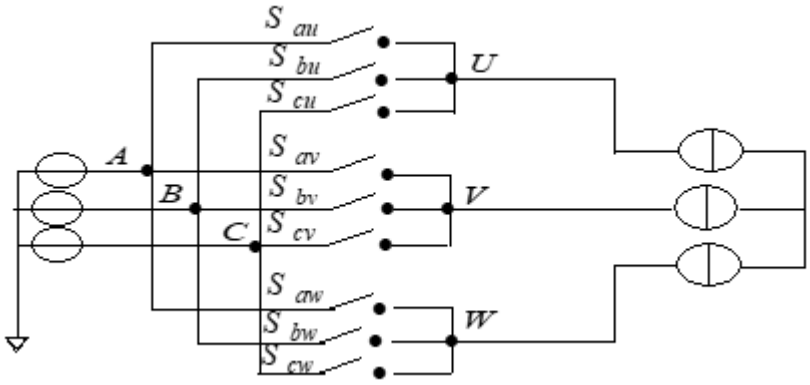

Source: Authors (Maafa *et al*., 2024)

The switch S_{ij} shown in Figure 1 is operated using the following switching function

$$S_{ij} = \begin{cases} 1 & S_{ij} \text{ is closed} \\ 0 & S_{ij} \text{ is open} \end{cases} \qquad i \in \{A,B,C\},\ j \in \{U,V,W\}, \qquad (1)$$

The restrictions (constraints) mentioned above can be stated as follows:

$$S_{Aj} + S_{Bj} + S_{Cj} = 1 \qquad j \in \{U,V,W\}, \qquad (2)$$

3 INDIRECT SVM METHOD

In order to use the space vector PWM, an imaginary direct current (DC) link is used to connect the modeled two-stage converter MC. The two stages behave

as follows: 1- Input rectifier with current connection, 2- As an inverter output voltage source (Filho *et al*., 2006).

Figure 3. Electrical and mechanical coupling for two IGs equivalent of the CDFIG

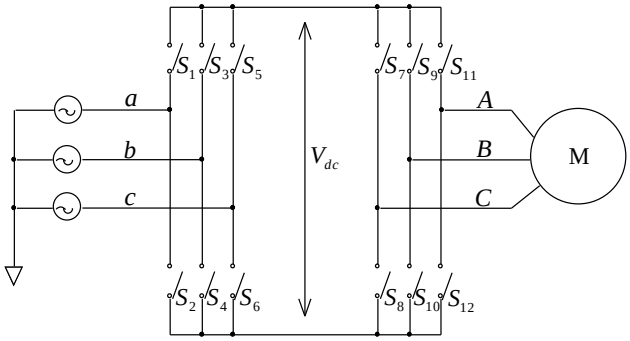

Source: Authors (Maafa *et al*., 2022)

The transfer function of MC can be represented as:

$$\begin{bmatrix} V_A \\ V_B \\ V_C \end{bmatrix} = \begin{bmatrix} S_7S_1 + S_8S_2 & S_7S_3 + S_8S_4 & S_7S_5 + S_8S_6 \\ S_9S_1 + S_{10}S_2 & S_9S_3 + S_{10}S_4 & S_9S_5 + S_{10}S_6 \\ S_{11}S_1 + S_{12}S_2 & S_{11}S_3 + S_{12}S_4 & S_{11}S_5 + S_{12}S_6 \end{bmatrix} \cdot \begin{bmatrix} V_a \\ V_b \\ V_c \end{bmatrix} \quad (3)$$

3.1 SVM FOR THE RECTIFIER STAGE

Using the transformation, the input current space vector I_{in} can be expressed as a space vector

$$I_{in} = \frac{2}{3}(I_a + I_b e^{j\frac{2\pi}{3}} + I_c e^{-j\frac{2\pi}{3}}) \quad (4)$$

Figure 4. Synthesis of reference current vector

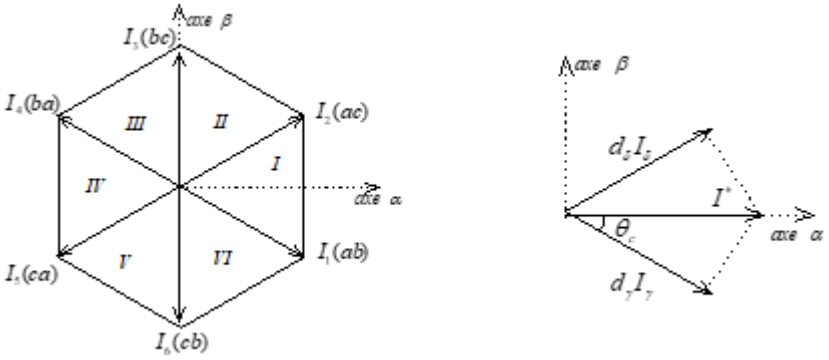

Source: Authors (Maafa *et al*., 2023)

The adjacent switching vectors *I*γ and *I*δ are impressed with the duty cycles *d*γ and *d*δ respectively *by* synthesizing *I**

$$I^* = d_\gamma I_\gamma + d_\delta I_\delta \tag{5}$$

With:

$$\begin{cases} d_\gamma = m_c \sin(\frac{\pi}{3} - \theta_i) \\ d_\delta = m_c \sin(\theta_i) \\ d_0 = 1 - (d_\gamma + d_\delta) \end{cases} \tag{6}$$

Where:

m_c: current modulation index (set to be unity).

θ_i: reference input angle of the vector (within its sector).

3.2 SVM FOR THE INVERTER STAGE

The vector of output voltage is defined as follows:

$$V_{out} = \frac{2}{3}(V_A + V_B e^{j\frac{2\pi}{3}} + V_C e^{-j\frac{2\pi}{3}}) \tag{7}$$

As shown in Figure 5, a hexagon is used in the complex plane as a shape to form the seven discrete space vectors.

Figure 5. Output voltage modulation for rectification stage

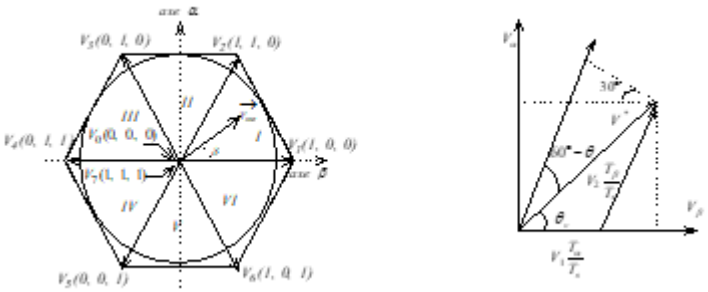

Source: Authors (Maafa *et al*., 2023)

The adjacent switching vectors v_α and v_β are impressed with the duty cycles d_α and d_β, respectively *by* synthesizing the space vector of the reference output voltage

$$V^* = d_\alpha v_\alpha + d_\beta I_\beta \quad (8)$$

The active vectors and their duty cycle are calculated as follows:

$$\begin{cases} d_\alpha = \frac{T_\alpha}{T_v} = m_v \sin(\frac{\pi}{3} - \theta_v) \\ d_\beta = \frac{T_\beta}{T_v} = m_v \sin(\theta_v) \\ d_0 = \frac{T_0}{T_v} = 1 - (d_\alpha + d_\beta) \end{cases} \quad (9)$$

Where:

θ_v : reference voltage vector angle (within the actual hexagon sector).

m_V: voltage modulation index (defines the desired voltage transfer ratio)

3.3 SVM FOR THE ENTIRE MATRIX CONVERTER

There is an imperative here to use a single modulation method that allows the independent space vector modulations to be combined into the nine bidirectional matrix converters.

$$\begin{cases} d_{\alpha\gamma} = d_\alpha . d_\gamma = m_v \sin(\frac{\pi}{3} - \theta_i).\sin(\frac{\pi}{3} - \theta_v) \\ d_{\alpha\delta} = d_\alpha . d_\delta = m_v \sin(\theta_i).\sin(\frac{\pi}{3} - \theta_v) \\ d_{\beta\delta} = d_\beta . d_\delta = m_v \sin(\theta_i).\sin(\theta_v) \\ d_{\beta\gamma} = d_\beta . d_\gamma = m_v \sin(\theta_v).\sin(\frac{\pi}{3} - \theta_i) \end{cases} \quad (10)$$

The zero vector is applied simultaneously with the remaining part of the switching period T_S

$$d_0 = 1 - (d_{\alpha\gamma} + d_{\alpha\delta} + d_{\beta\gamma} + d_{\beta\gamma\delta}) \quad (11)$$

The optimized indirect SVM switching sequence is listed in Table 1

Table 1: Switching sequence for voltage sector = I, current sector = I.

$\beta\gamma$	$\alpha\gamma$	$\alpha\delta$	$\beta\delta$	0	$\beta\delta$	$\alpha\delta$	$\alpha\gamma$	$\beta\gamma$
abb	*aba*	*aca*	*acc*	*ccc*	*acc*	*aca*	*aba*	*abb*
$T_{\beta\gamma}/2$	$T_{\alpha\gamma}/2$	$T_{\alpha\delta}/2$	$T_{\beta\delta}/2$	T_0	$T_{\beta\delta}/2$	$T_{\alpha\delta}/2$	$T_{\alpha\gamma}/2$	$T_{\beta\gamma}/2$
V_1-I_1	V_6-I_1	V_6-I_2	V_1-I_2	V_0-I_0	V_1-I_2	V_6-I_2	V_6-I_1	V_1-I_1

Source: Authors.

4 MODEL AND CONTROL OF CDFIG

The two induction generators with pole-pairs respectively p_1 and p_2 are the most important components of the cascaded doubly fed induction generator (CDFIG), in the traditional doubly fed induction machine (DFIM), for eliminating the copper rings and brushes, they are connected in cascade (Maafa *et al*., 2016). The electrical and mechanical coupling of two wound rotors is shown in Figure 6.

Figure 6. Electric and mechanical coupling of two IG equivalent of the CDFIG

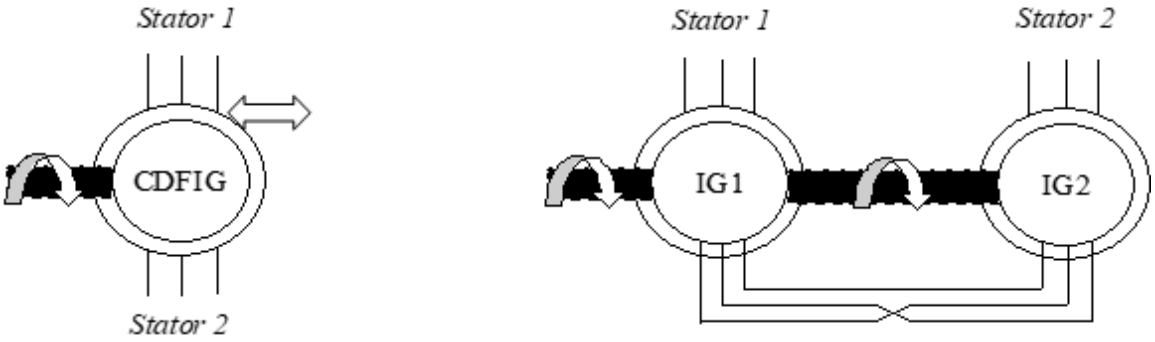

Source: Authors

In a synchronously rotating d–q frame, the machines equations written are:

- The machine 1:

$$\begin{cases} v_{ds1} = R_{s1} i_{ds1} + \dfrac{d}{dt}\varphi_{ds1} - \omega_s \varphi_{qs1} \\ v_{qs1} = R_{s1} i_{qs1} + \dfrac{d}{dt}\varphi_{qs1} + \omega_s \varphi_{ds1} \\ v_{dr1} = R_{r1} i_{dr1} + \dfrac{d}{dt}\varphi_{dr1} - (\omega_s - \omega_{r1})\varphi_{qr1} \\ v_{qr1} = R_{r1} i_{qr1} + \dfrac{d}{dt}\varphi_{qr1} + (\omega_s - \omega_{r1})\varphi_{dr1} \end{cases} \quad (12)$$

- The machine 2:

$$\begin{cases} v_{dr2} = R_{r2} i_{dr2} + \dfrac{d}{dt}\varphi_{dr2} - (\omega_s - \omega_{r1})\varphi_{qr2} \\ v_{qr2} = R_{r2} i_{qr2} + \dfrac{d}{dt}\varphi_{qr2} + (\omega_s - \omega_{r1})\varphi_{dr2} \\ v_{ds2} = R_{s2} i_{ds2} + \dfrac{d}{dt}\varphi_{ds2} - (\omega_s - \omega_{r1} - \omega_{r2})\varphi_{qs2} \\ v_{qs2} = R_{s2} i_{qs2} + \dfrac{d}{dt}\varphi_{qs2} + (\omega_s - \omega_{r1} - \omega_{r2})\varphi_{ds2} \end{cases} \quad (13)$$

The rotor and stator fluxes of CDFIG can be expressed as:

$$\begin{cases}\Phi_{ds1}=L_{s1}i_{ds1}+L_{m1}i_{dr}\\ \Phi_{qs1}=L_{s1}i_{qs1}+L_{m1}i_{qr}\\ \Phi_{dr1}=L_{r1}i_{dr}+L_{m1}i_{ds1}\\ \Phi_{qr1}=L_{r1}i_{qr}+L_{m1}i_{qs1}\end{cases} \text{ and } \begin{cases}\Phi_{ds2}=L_{s2}i_{ds2}-L_{m2}i_{dr}\\ \Phi_{qs2}=L_{s2}i_{qs2}-L_{m2}i_{qr}\\ \Phi_{dr2}=-L_{r2}i_{dr}+L_{m2}i_{ds2}\\ \Phi_{qr2}=-L_{r2}i_{qr}+L_{m2}i_{qs2}\end{cases} \quad (14)$$

The electrical connection coupling between the two rotors is modeled as follows:

$$\begin{cases}v_{\mathrm{dr1}}= \ v_{\mathrm{dr2}}=v_{\mathrm{dr}}\\ v_{\mathrm{qr1}}= \ v_{\mathrm{qr2}}=v_{\mathrm{qr}}\end{cases} \text{ and } \begin{cases}\mathrm{i}_{\mathrm{dr1}}=-\mathrm{i}_{\mathrm{dr2}}=\mathrm{i}_{\mathrm{dr}}\\ \mathrm{i}_{\mathrm{qr1}}=-\mathrm{i}_{\mathrm{qr2}}=\mathrm{i}_{\mathrm{qr}}\end{cases} \quad (15)$$

The circuits of the rotors are connected in such a way that the couples are added:

$$T_e=p_1.L_{m1}\left(i_{dr}.i_{qs1}-i_{ds1}.i_{qr}\right)+p_2.L_{m2}\left(i_{dr}.i_{qs2}-i_{ds2}.i_{qr}\right) \quad (16)$$

The reactive and active powers for those provide for grid as well as at both stators 1 and 2 are written as:

$$\begin{cases}P_{s1}=v_{ds1}.i_{ds1}+v_{qs1}.i_{qs1}\\ Q_{s1}=v_{qs1}.i_{ds1}-v_{ds1}.i_{qs1}\end{cases} \quad (17)$$

$$\begin{cases}P_{s2}=v_{ds2}.i_{ds2}+v_{qs2}.i_{qs2}\\ Q_{s2}=v_{qs2}.i_{ds2}-v_{ds2}.i_{qs2}\end{cases} \quad (18)$$

$$\begin{cases}P_g=P_{s1}+P_{s2}\\ Q_g=Q_{s1}+Q_{gs2}\end{cases} \quad (19)$$

The reference frame d-q is chosen where the d-axis is aligned with the stator 01 flux and quadrature component of stator 01 flux is zero (Ghedamsi *et al*., 2010).

$$\begin{cases}\varphi_{ds1}=\varphi_{\mathrm{s1}}\\ \varphi_{qs1}=0\end{cases} \quad (20)$$

Then the torque is simplified into:

$$T_e = p_1\varphi_{s1}i_{qs1} + p_2(\varphi_{ds2}i_{qs2} - \varphi_{qs2}i_{ds2}) \quad (21)$$

Neglecting the resistance of stator 1 R_{s1}, it can be expressed:

$$\begin{cases} v_{ds1} = 0 \\ v_{qs1} = V_s = \omega_s.\varphi_{s1} \end{cases} \quad (22)$$

The voltages of stator 2, the reactive and active powers of stator, can be expressed depending on the rotor currents as:

$$\begin{cases} v_{ds2} = R_{s2}i_{ds2} + (L_{s2} - CL_{m2})\dfrac{di_{ds2}}{dt} - s.\omega_s(L_{s2} - CL_{m2})i_{qs2} \\ v_{qs2} = R_{s2}i_{qs2} + (L_{s2} - CL_{m2})\dfrac{di_{qs2}}{dt} + s.\omega_s(L_{s2} - CL_{m2})i_{ds2} + s.\dfrac{L_{m1}V_s}{L_{s1}} \end{cases} \quad (23)$$

$$\begin{cases} P_{s1} = -C.V_s\dfrac{L_{m1}}{L_{s1}}i_{qs2} \\ Q_{s1} = \dfrac{V_s^2}{\omega_s.L_{s1}}\left(1 + \dfrac{C.L_{m1}^2}{L_{s1}.L_{m2}}\right) - C.V_s\dfrac{L_{m1}}{L_{s1}}i_{ds2} \end{cases} \quad (24)$$

With: $s = \dfrac{\omega_s - (p_1 + p_2)\Omega_r}{\omega_s}$ and $C = \dfrac{L_{m2}}{L_{r1} + L_{r2} - \dfrac{L_{m1}^2}{L_{s1}}}$

For both equations in (23), the second derivative terms are nulls in steady state. Because of their weak impact and influence, the third terms can be neglected, as they are cross-coupling.

5 SIMULATION RESULTS AND DISCUSSION

A direct connection of the CDFIG to the electric grid via the stator 1 is simulated in this section, therefore an AC/AC direct converter is controlled via its stator 2 circuit.

After the optimum mechanical power of the turbine was set, the simulation

results were obtained for an active reference power P_{s1_re} =1,5 MW and reactive reference power Q_{s1_ref} = 0MVar, The details of the CDFIG parameters exploited in this simulation are presented in the Appendix A. In order to reduce the loads and ensure the generation of maximum energy, the considered system is controlled.

The optimal mechanical power is obtained as a result of the rotor speed of the CDFIG, which is shown in Figure 7. CDFIG sliding is illustrated in Figure 8. The reactive and active powers for the stator 1 is given in Figure 9.The powers in stator 1 follow their track of references in excellent way. The reactive and active powers for the stator 2 is given in Figure 10. As it is clear for the figure, it is shown at a hyper-synchronous operation mode the active power values up 1.5 MW is transferred from the stator 2 side. Figure 11. (a). shows the reactive and active powers of the power grid. In contrast, the Figure 11. (b) shows the zoom waveforms of the current and voltage, it is clear from figure that the voltage is in opposite phase with respect to the sinusoidal current, meaning that the electrical grid is supplied with purely active energy from CDFIG.

Figure 7. Rotor speed

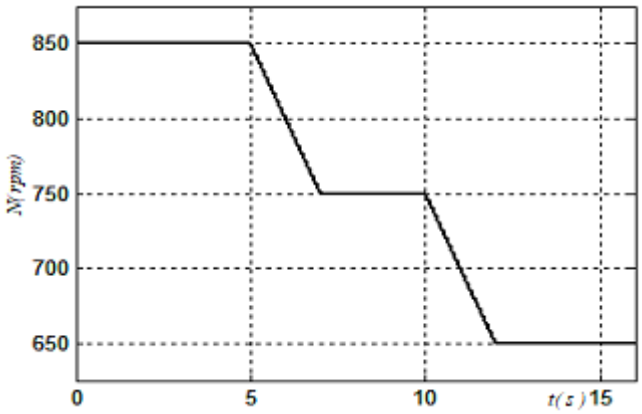

Source: Authors

Figure 8.CDFIG slip

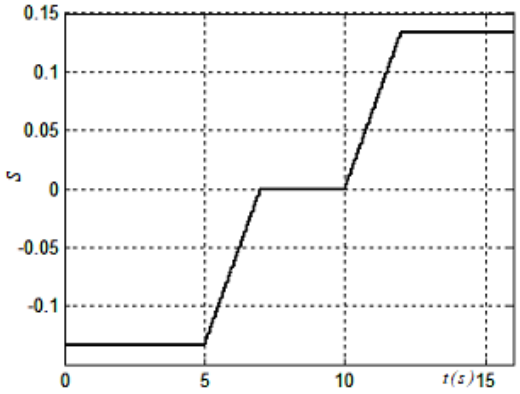

Source: Authors

Figure 9 . Reactive and active powers of stator 2.

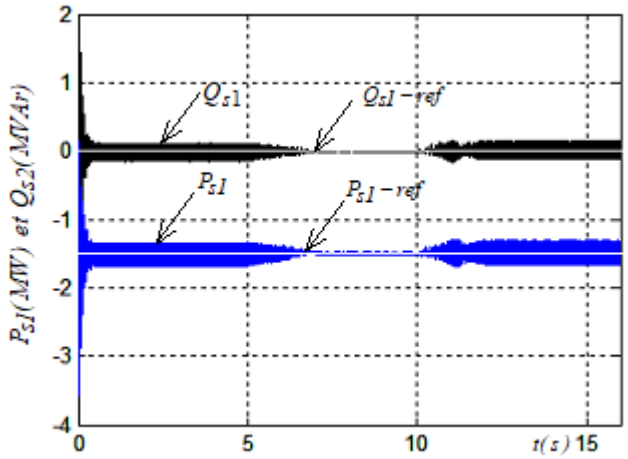

Source: Authors

Figure 10. Reactive and active powers of stator 2.

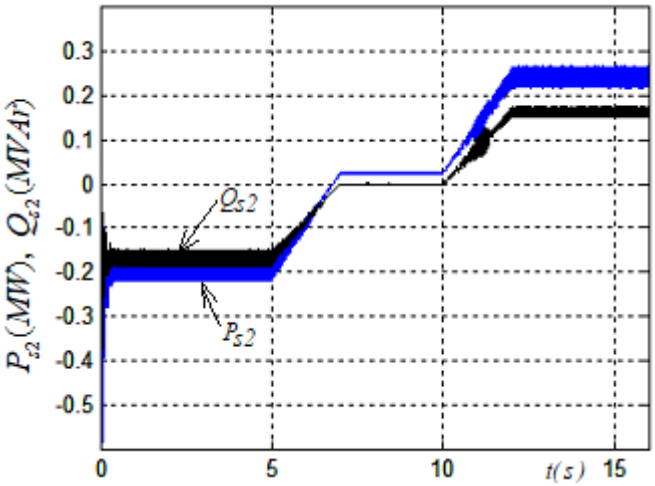

Source: Authors

Figure 11 . (a): grid active and reactive powers. (b): grid current and voltage (Zoom).

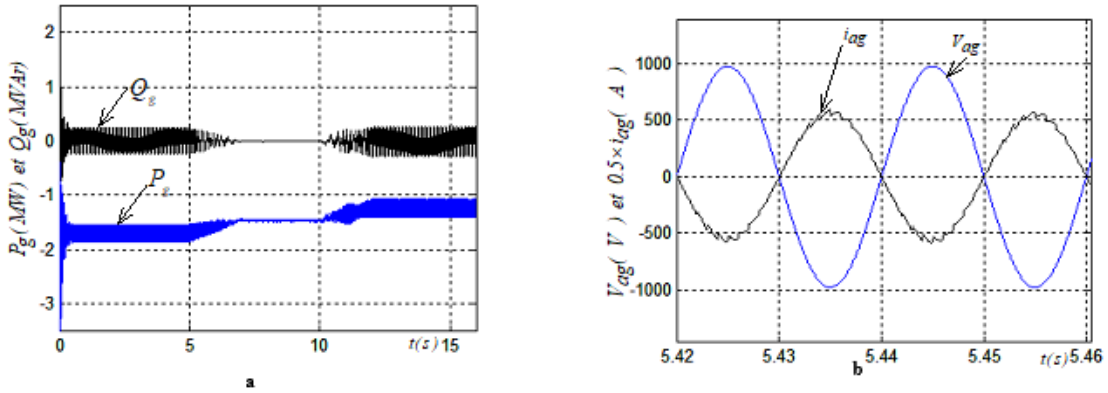

Source: Authors

The current and voltage waveforms of the stator 1 are shown in Figure 12. (a) it is clear from figure that the voltage is in opposite phase with respect to the sinusoidal current (Figure 12. (b)).

The current and voltage waveforms of the stator 2 are shown in Figure 13. (a). As shown in (Figure 13. (a) and Figure 13. (c)), and according to the slips, the frequency of this current and voltage varies. For s = 0, the current and voltage waveforms of stator 2 are continuous (Figure 13. (d)). Figure 14. present the waveforms of the plotted three-phase rotor currents. For synchronous operation mode i.e. s = 0, the current waveforms are continuous. Figure 15 gives rotor current waveforms for s=0, its shows clearly that the rotor waveforms frequency are equal to 25 Hz.

Figure 12 . (a) current and voltage of stator 1. (b) current and voltage of stator 1 (Zoom)

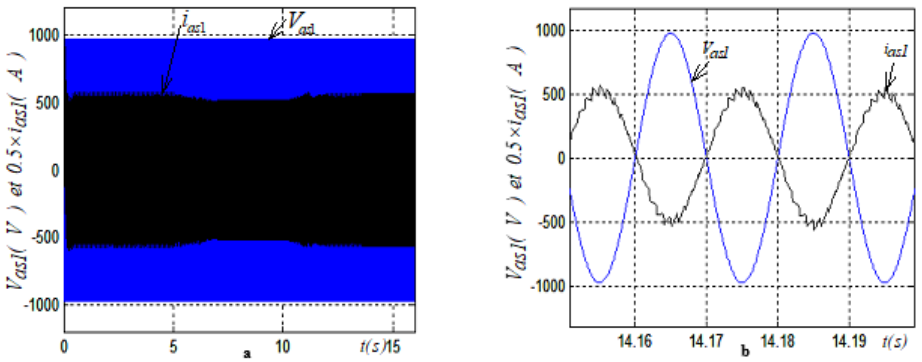

Source: Authors

Figure 13. (a): current and voltage of stator 2. (b): current and voltage of stator 2 (Zoom for s<0). (c): current and voltage of stator 2 (Zoom for s>0). (d): current and voltage of stator 2 (Zoom for s = 0).

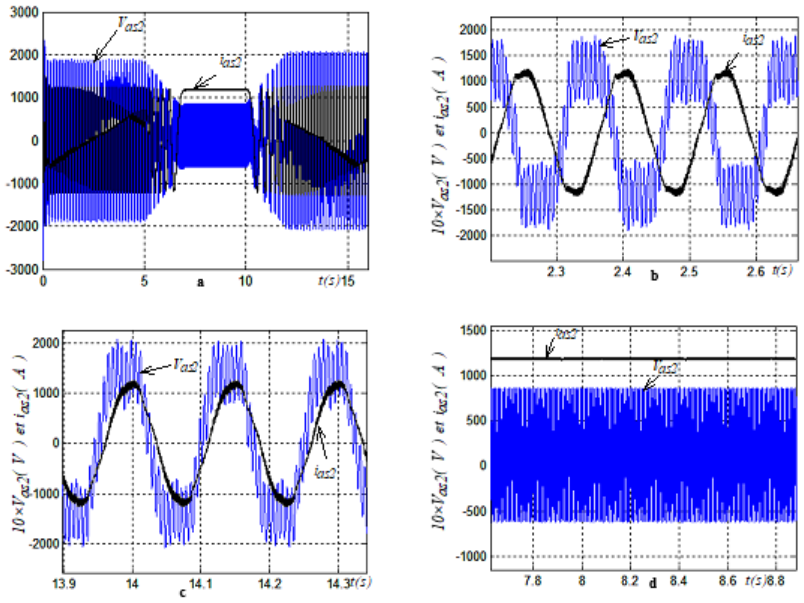

Source: Authors

Figure 14. currents of stator 2 in sub-synchronous, synchronous, and hyper-synchronous

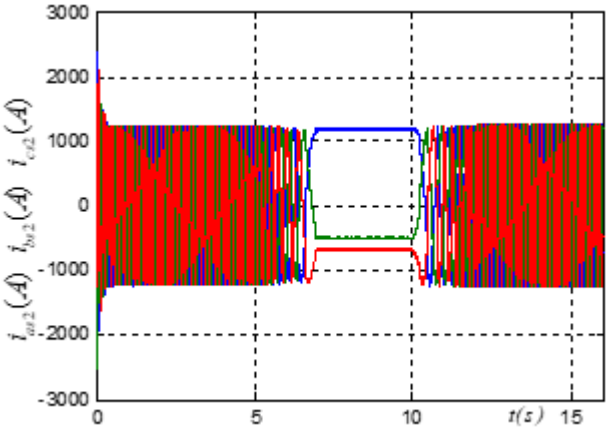

Source: Authors

Figure 15 . Rotor currents for S=0.

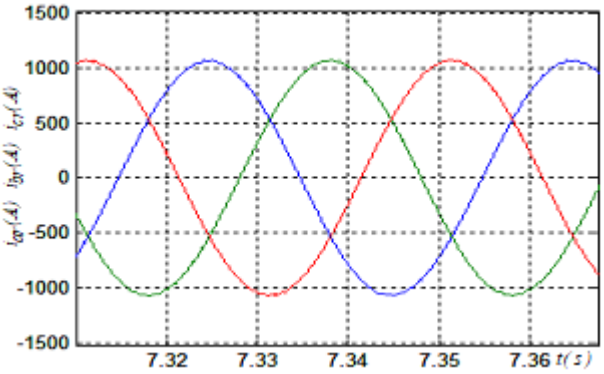

Source: Authors

5 CONCLUSIONS

In this paper, a three level sparse matrix converter related to variable speed wind generator (VSWG) is presented.

In the two-quadrant situation, the CDFIG is worked. For s>0, the CDFIG operate in the sub-synchronous situation. For s<0, the CDFIG is work in the super-synchronous process. For s=0, the CDFIG is run as a synchronized asynchronous generator, and for the stator 2, the frequency of currents and voltages evaluates to zero.

From the simulation, the results confirm that reactive and active powers follow the path of their own reference values in a very good way. In order to achieve an input power factor, close to unity, the input power factor for the matrix converter is controlled.

In the matrix converter there is no energy storage element and thus leads to extending the life of the proposed structure and maintaining it, and the use of CDFIG allows elimination of brushes and copper rings, which will further reduce the cost of maintenance of traditional DFIG.

The study concludes that the integration of a matrix converter with a CDFIG system offers substantial benefits in terms of performance and reliability. Future work will focus on experimental validation and optimization of control strategies to further enhance system efficiency.

APPENDIX: PARAMETERS

CDFIG: The two machines used, are identical:

P=1.5 MW; V=690 V ; $p_1=p_2=2$; $f_1=f_2=0.0071$ N.m.s/rad; $J_1=J_2=50$ kg.m^2.

$R_{s1}=R_{s2}=0.012\ \Omega$; $R_{r1}=R_{r2}=0.021\ \Omega$;

$L_{s1}=L_{s2}=0.0137$ H ;$L_{r1}=L_{r2}=0.0137$ H ; $L_{m1}=L_{m1}=0.0135$ H;

REFERENCES

BAROTE, L. *et al*. Energy storage for a stand-alone wind energy conversion system. **Revue Roumaine des Sciences Techniques- sries Électrotechniques et Énergergitiques**, v. 55, 3, p. 235–242, 2010. Available at : http://revue.elth.pub.ro/viewpdf.php?id=236.

CHEKKAL, S. *et al*. Fuzzy logic control strategy of wind generator based on the dual-stator induction generator. **Electrical Power and Energy Systems**, v. 59, p. 166-175, 2014. doi : https://doi.org/10.1016/j.ijepes.2014.02.005.

MAAFA, A. *et al*. Cascaded doubly fed induction generator with variable pitch control system. **Revue Roumaine des Sciences Techniques- sries Électrotechniques et Énergergitiques**, v. 61, 4, p. 361-366, 2016. Available at : http://revue.elth.pub.ro/upload/10474409_AMaafa_RRST_4_2016_pp_361-366.pdf.

El Achkar, M. *et al*. Generic study of the power capability of a cascaded doubly fed induction machine. **Electrical Power and Energy Systems**, v. 86, p. 61-70, 2017. doi: https://doi.org/10.1016/j.ijepes.2016.09.011.

KOSTYANTYN, P.; DEWEI, X. Modeling and Control of Brushless Doubly-Fed Induction Generators in Wind Energy Applications. *In:* **APEC 07 - Twenty-Second Annual IEEE Applied Power Electronics Conference and Exposition,** 2008, p. 1191–97. doi: 10.1109/APEX.2007.357565.

MOAZEN, M. *et al.* Mathematical modeling and analysis of brushless doubly fed reluctance generator under unbalanced grid voltage condition. **Electrical Power and Energy Systems**, v. 83, p. 547-559, 2016, doi: https://doi.org/10.1016/j.ijepes.2016.04.050.

ADAMOWICZ, M.; STRZELECKI, R. Cascaded Doubly Fed Induction Generator for Mini and Micro Power Plants Connected to Grid. *In:* **2008 13th International Power Electronics and Motion Control Conference,** 2008, p. 1927–33, doi: 10.1109/EPEPEMC.2008.4635516.

TAIB, N. *et al.* Performance and efficiency control enhancement of wind power generation system based on dfig using three-level sparse matrix converter, **Electrical Power and Energy Systems**, v. 53, p. 287-296, 2013. doi: https://doi.org/10.1016/j.ijepes.2013.05.019.

MOHAN, N. *et al.* Power Electronics: Converters. **Applications, and Design. Hoboken, NJ: John Wiley & Sons**, 2003. Available at : https://www.sciencedirect.com/topics/engineering/power-electronic-converter.

ALESINA, A.; VENTURINI, M. Analysis and Design of Optimum-Amplitude Nine-Switch Direct AC-AC Converters. **IEEE Transactions on Power Electronics**, v. 4, 1, p. 101-112, 1989. doi: 10.1109/63.21879.

BENACHOUR, A. *et al*. A new direct torque control of induction machine fed by indirect matrix converter. **Revue Roumaine des Sciences Techniques- sries Électrotechniques et Énergergitiques**, v. 62, 1, p. 25-30, 2017. Available at : http://revue.elth.pub.ro/upload/82006305_ABenachour_RRST_1_2017_pp_25-30.pdf.

YUE, F. *et al*. Relationship of modulation schemes for matrix converters. *In:* **3rd IET International Conference on Power Electronics, Machines and Drives (PEMD)**, 2007, p. 266-270. Available at : https://ieeexplore.ieee.org/document/4123527?denied=.

CASADEI, D. *et al*. Space vector control of matrix converters with unity input power factor and sinusoidal input/output waveforms. In: **IEE Proceedings of Fifth European Conference on Power Electronics and Applications**, 1993, p. 13-16. Available at : https://ieeexplore.ieee.org/document/265052.

HUBER, L. *et al*. Space vector modulated three phase to three phase matrix converter with input power factor correction. **IEEE Transactions on Industry Application**, v. 31, 6, p. 1234-46, 1995, doi: 10.1109/28.475693.

MAAFA, A. *et al*. Performance improvement of a DPC-FPID strategy with matrix converter using CDFIG. **Wind power system. Wind Engineering,** 2024 doi:10.1177/0309524X241267742.

FILHO, M. E. O. *et al*. A simple current control for matrix converter. In: **Conference Record of the 2006 IEEE Industry Applications Conference Forty-First IAS Annual Meeting**, 2006 Available at: 10.1109/IAS.2006.256823.

MAAFA, A. *et al*. Improvement of Sliding Mode Control Strategy Founded on Cascaded Doubly Fed Induction Generator Powered by a Matrix Converter. **Engineering, Technology & Applied Science Research,** v. 12, 5, p. 9217-9223, 2022. doi: https://doi.org/10.48084/etasr.5166.

MAAFA, A. *et al*. Optimization of the Powers Exchanged between a Cascaded Doubly Fed Induction Generator and the Grid with a Matrix Converter. **The Eurasia Proceedings of Science Technology Engineering and Mathematics,** v. 26, p. 700-709, 2023. doi: https://doi.org/10.55549/epstem.1412495.

GHEDAMSI, K.; AOUZELLAG, D. Improvement of the performances for wind energy conversions systems. **Electrical Power and Energy Systems**, v. 32, p. 936-945, 2010. doi: https://doi.org/10.1016/j.ijepes.2010.02.012.